MINERALOGY FROM GEOCHEMICAL WELL LOGGING

Michael M. Herron

Schlumberger-Doll Research, Old Quarry Road, Ridgefield, Connecticut 06877

Abstract—Multivariate statistical analyses of geochemical, mineralogical, and cation-exchange capacity (CEC) data from a Venezuelan oil well were used to construct a model which relates elemental concentrations to mineral abundances. An r-mode factor analysis showed that most of the variance could be accounted for by four independent factors and that these factors were related to individual mineral components: kaolinite, illite, K-feldspar, and heavy minerals. Concentrations of Al, Fe, and K in core samples were used to estimate the abundances of kaolinite, illite, K-feldspar, and, by subtraction from unity, quartz. Concentrations of these elements were also measured remotely in the well by geochemical logging tools and were used to estimate these mineral abundances on a continuous basis as a function of depth. The CEC was estimated from a linear combination of the derived kaolinite and illite abundances. The formation's thermal neutron capture cross section estimated from the log-derived mineralogy and a porosity log agreed well with the measured data. Concentrations of V, among other trace elements, were modeled as linear combinations of the clay mineral abundances. The measured core V agreed with the derived values in shales and water-bearing sands, but exceeded the clay-derived values in samples containing heavy oil. The excess V was used to estimate the V content and API Gravity of the oil. The log-derived clay mineralogy was used to help distinguish nonmarine from transitional depositional environments. Kaolinite was the dominant clay in nonmarine deposits, whereas transitional sediments contained more illite.

Key Words—Elemental analysis, Illite, Kaolinite, Mineralogical analysis, Multivariate analysis, Neutron capture cross section, Well logging.

INTRODUCTION

Formation evaluation in the petroleum industry would be significantly enhanced if it were possible to determine the mineralogy in a given well or field without the time and expense of collecting and analyzing core samples. Such mineralogical information could help in reservoir quality evaluation, production risk analysis, depositional environment interpretation, and well-to-well correlation. Currently, geophysical logs are usually interpreted in terms of general lithology, such as sandstone, shale, or limestone, but only rarely in terms of specific mineral phases. Geochemical logs, i.e., wireline measurements of total chemical concentrations on a continuous basis with depth, offer one possibility for obtaining more accurate mineral information.

The use of total chemical composition to estimate mineral abundances is a common practice in igneous petrology, but has met with only limited success in sedimentary rocks (Imbrie and Poldervaart, 1959; Miesch, 1962; Pearson, 1978; Gold *et al.,* 1983). The primary causes of disagreement between calculated and measured mineral abundances are the presence of additional minerals beyond those included in the models and the variability in chemical composition of clay minerals due to ionic substitution and ionic adsorption. At least some of this chemical variability, e.g., Fe in kaolinites, has been linked to the degree of disorder or the "crystallinity" of the clay structure (Mestdagh *et al.,* 1980; Brindley *et al.,* 1986). Such variability in

composition may be less significant when considering samples from a single geologic setting.

This report examines the correlations between chemical composition and mineral abundances in the MFM-7S well in the Faja Petrolifera del Orinoco in eastern Venezuela. The well penetrates a deltaic—alluvial to brackish water—sequence of the Oficina Formation composed of unconsolidated sands and muds containing abundant heavy oil (Everett *et al.,* 1983; Pirie and Everett, 1984). This study focuses on the 460–580-m depth interval from which 114 sidewall core samples were obtained.

METHODS

Interior portions of the sidewall cores, visibly free of drilling mud, were split into several aliquots. A 1-g sample was analyzed for elemental composition by instrumental neutron activation analysis (INAA) at the Atomic Energy of Canada, Ltd. reactor facility. Twenty-one elements were consistently detected and used for the geochemical data base. The remaining sample aliquots were cleaned of hydrocarbons by successive treatments of toluene, acetone, and chloroform in a Soxhlet apparatus. Many of these cleaned samples were also analyzed by INAA.

The cation-exchange capacities (CEC) of the cleaned aliquots were measured using NH_4^+ as the exchanging cation, Kjeldahl distillation, and final detection by titration (Ridge, 1983). The <20-μm size fraction was separated by centrifuge techniques. Mineralogy of the

bulk and fine fraction was determined by X-ray powder diffraction (XRD) on a Philips diffractometer using CuKα radiation with a theta-compensating slit. Bulk analyses were made of randomly oriented samples; the <20-μm fraction was oriented by filtration and transferred onto a silicon wafer. Counts were obtained for 1 s at 0.04°2θ intervals. The XRD results were quantified using mixtures of mineral standards of suitable crystallinity to establish a peak height-weight fraction relationship. Patterns were made after air-drying, glycolation, and heating (400° and 550°C). Only two clay minerals, kaolinite and illite, were prominent in these samples; the illite commonly exhibited a small, unquantified, degree of swelling after glycolation indicating trace quantities of smectite. Quartz and K-feldspar were also abundant. About 2% siderite and/or pyrite were detected in many shale samples and these minerals accounted for less than 20% of the total iron.

As part of a separate study on the relationship between crystallinity and trace element content, eight samples of Georgia kaolinites were supplied by J. L. Harrison of the Georgia Kaolin Research Company. These samples, also studied by Brindley et al. (1986), were analyzed by INAA; exchangeable cations were then replaced by NH_4^+ as in the CEC procedure and the samples were reanalyzed by INAA.

Continuous chemical analyses were obtained from three geochemical well logging tools. The Natural Gamma-Ray Spectroscopy Tool (NGT[1]) measures the natural gamma ray activity due to potassium and daughter products of thorium and uranium. The output response is in terms of the weight percentage of the elements. The Gamma-Ray Spectrometry Tool (GST[1]) measures gamma rays induced by neutron-element interactions. The GST responds to Fe, Si, Ca, S, Cl, and H. The thermal neutron capture cross section of the formation was also measured. The Enhanced Resolution Tool (ERT[1]) is an experimental tool which is capable of making NGT and GST measurements as well as downhole neutron activation analyses. An intrinsic germanium detector is used in the tool to provide high resolution of gamma ray energies. The ERT was used in this well to measure Al concentrations by neutron activation.

RESULTS AND DISCUSSION

Element-mineral relationships

The determination of the quantitative relationship between elemental concentrations and mineralogy consisted of two steps. The first step was a factor analysis of the concentrations of 21 elements, the abundances of four minerals, the CEC values, and the amounts of the <20-μm fractions. The second step was a multiple

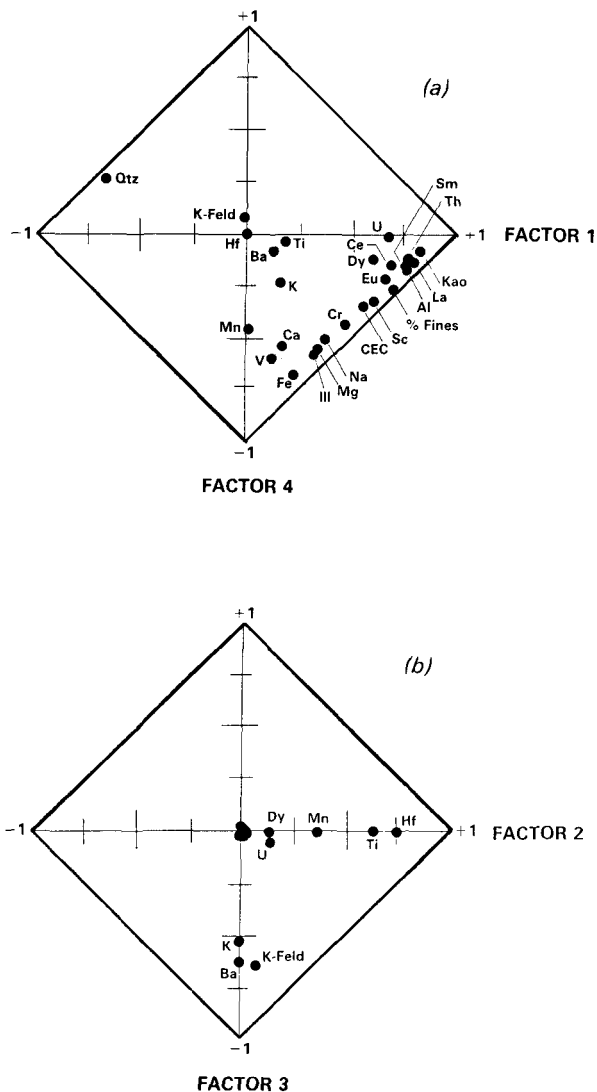[1] Trademark of Schlumberger.

Figure 1.   The r-mode factor analysis results. Points for each variable represent fraction of total variance associated with each factor. (a) factor 1 (kaolinite) vs. factor 4 (illite); (b) factor 2 (heavy minerals) vs. factor 3 (K-feldspar).

regression analysis of selected elements and minerals in order to construct a model.

An r-mode factor analysis with varimax rotation (Davis, 1973) was performed on the data set to establish correlations between the variables. Four factors were retained prior to rotation using the criterion that the unrotated eigenvalues be greater than unity, i.e., that they account for more variance than that represented by the original input variables. These four factors accounted for 86% of the total variance. The elements of the rotated factor matrix, squared so that the values were proportional to the fractional variance explained for each variable, are plotted in Figure 1. The diamond border represents the maximum variance of

Table 1. Minimal-input model c_{ij} coefficients used to estimate abundances of kaolinite, illite, and K-feldspar.

Element (%)	Kaolinite	Illite	K-feldspar
Al	19	9.2	10.5
Fe	.14	10.6	.05
K	.35	4	12

each variable. Variables which plot near the border of the plot had most of their variance explained by, i.e., are associated with, the two factors involved; variables not associated with the two factors plotted near the origin.

Factors 1 and 4 correlated with the clay minerals, kaolinite and illite, respectively, and together accounted for 72% of the total variance (Figure 1a). Clay-related factors were expected to have the highest eigenvalues in such an analysis because, on average, most of the elements considered here are more highly concentrated in shales than in sandstones or carbonates (Turekian and Wedepohl, 1961). Factor 1, the kaolinite factor, was associated with Al, Th, U, the rare earth elements La, Sm, Eu, and Dy, and the kaolinite. Factor 4, the illite factor, was associated with Fe, V, Mg, Ca, Na, Cr, and to a lesser extent K, as well as with the illite. Some variables were associated with both factors, such as the CEC, the <20-μm fraction, and the element Sc. In addition, the quartz abundance was negatively correlated with both clay factors, demonstrating the inverse relationship between clay content and quartz content.

The matrix elements of factors 2 and 3 are shown in Figure 1b. Factor 3 is clearly associated with the K-feldspar and the elements K and Ba. A similar association between Ba and K-feldspar was noted by Tardy (1975). Factor 2 is associated primarily with Hf and Ti and less so with Mn, U, and Dy. None of the minerals determined by XRD were significantly associated with this factor. This suite of elements indicates that factor 2 might relate to heavy minerals such as zircon and rutile or anatase. Zircon is the primary source for Hf, whereas uranium and heavy rare earths, such as Dy, are relatively abundant in many zircons (Rankama and Sahama, 1950; Adams *et al.,* 1959; Murali *et al.,* 1983).

The strong associations of minerals and elements shown by the factor analysis suggests that the abundances of the primary minerals in this well may be estimated from concentrations of only three elements. The XRD results show that the major minerals were quartz, K-feldspar, kaolinite, and illite; other constituents were relatively rare. In matrix form, mineral abundances, [M], were solved from elemental concentrations, [E],

$$[E] = [C][M],$$

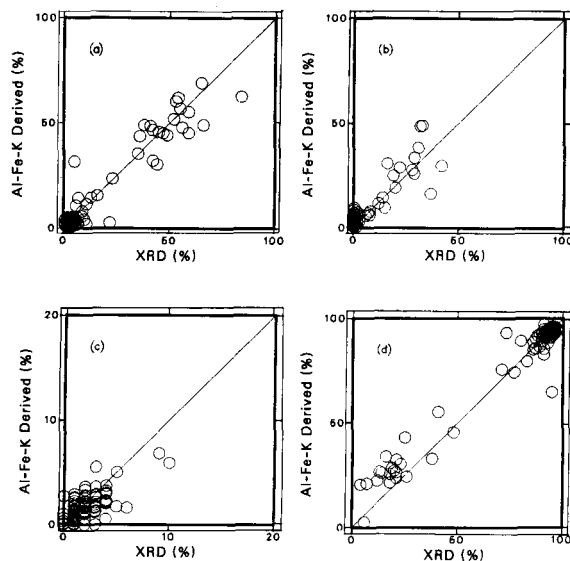where [C] is a coefficient matrix whose matrix ele-

Figure 2. Mineral abundances measured by X-ray powder diffraction (XRD) compared with estimated abundances derived from the minimal-input model and Al, Fe, and K concentrations: (a) kaolinite; (b) illite; (c) K-feldspar; (d) residual from model vs. quartz.

ments, c_{ij}, represent elemental concentrations in "pure end-member" minerals. This approach follows that of Pearson (1978) and Hodgson and Dudeney (1984) and was extended here to include non-clay phases. Only three elements were required to solve the abundances of kaolinite, illite, and K-feldspar. For each sample, if the sum of derived mineral abundances was less than unity, a residual mineral term was calculated. The residual phase was assumed to be quartz. This model was a minimal-input model that neglected the heavy mineral and smectite contributions. The elements Al, Fe, and K were chosen as the input variables on the basis of the factor analysis and because they were also measured in this well by the geochemical tools. The c_{ij} values were determined from the literature or by regression techniques using the data from this well and are given in Table 1. Mineral abundances are, of course, commonly correlated; thus, such a multiple regression approach does not always yield the most satisfactory values.

Figure 2 compares mineral abundances determined by XRD with values estimated from Al, Fe, and K concentrations. Derived abundances of kaolinite, by far the dominant clay mineral, agree closely with the XRD data. Derived illite abundances also agree with the XRD data, but some scatter reflects the impact of the smectite, siderite, and pyrite. The K-feldspar abundances are so low as to have a large relative error associated with the measurements. Nevertheless, the derived abundances generally agree with the measured values. Figure 2d shows that the derived residual min-
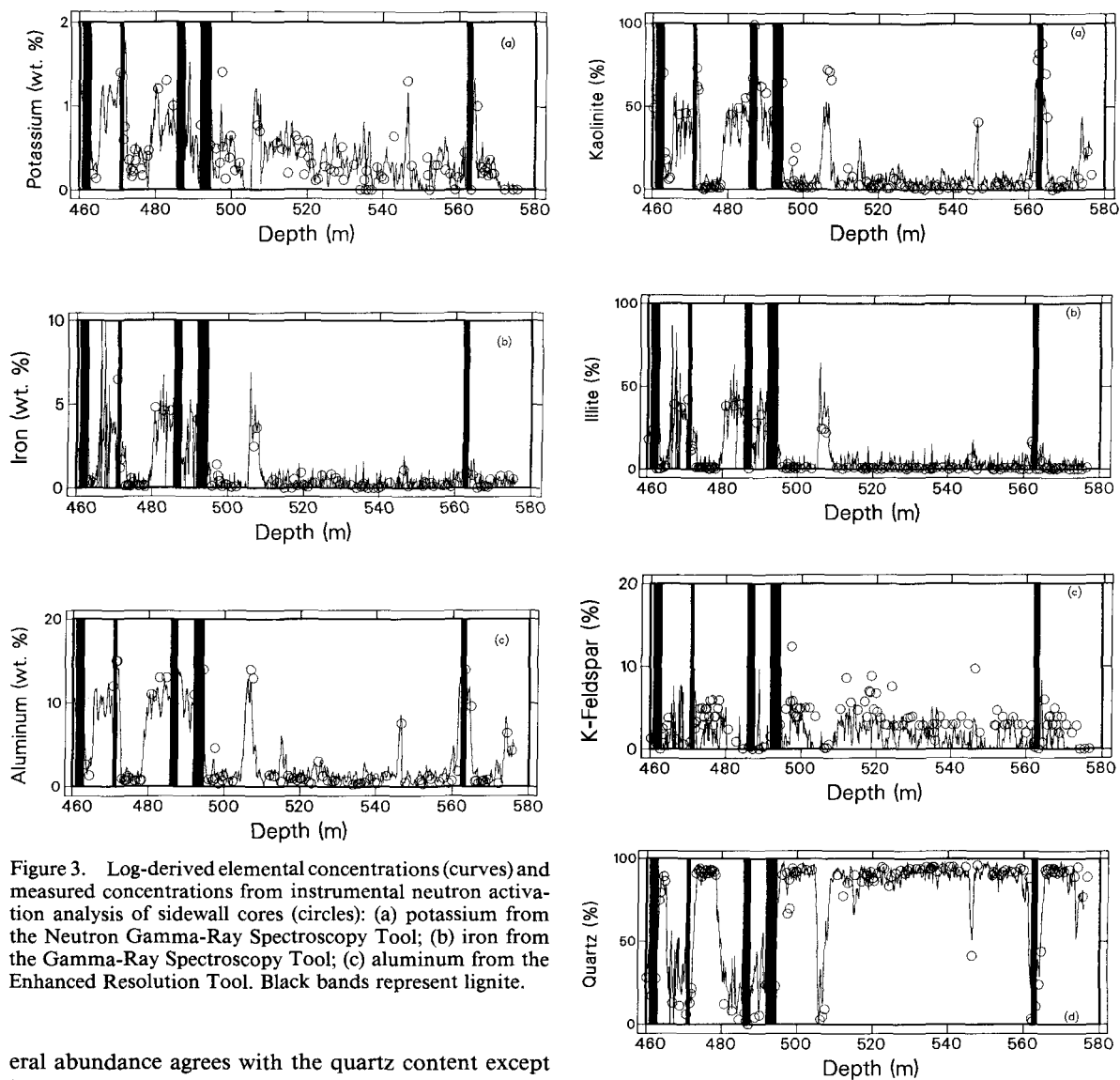
Figure 3. Log-derived elemental concentrations (curves) and measured concentrations from instrumental neutron activation analysis of sidewall cores (circles): (a) potassium from the Neutron Gamma-Ray Spectroscopy Tool; (b) iron from the Gamma-Ray Spectroscopy Tool; (c) aluminum from the Enhanced Resolution Tool. Black bands represent lignite.

Figure 4. Log-derived mineral abundances (curves) compared with sidewall core mineralogy (circles): (a) kaolinite; (b) illite; (c) K-feldspar; (d) residual from model and quartz. Black bands are lignite zones.

eral abundance agrees with the quartz content except in some of the low-quartz shales. The average absolute difference between measured and minimal-input model abundances is only 3.0% for kaolinite, 2.6% for illite, 0.9% for K-feldspar, and 3.5% for quartz. Thus, the chemically-derived abundances are reasonably good approximations of the XRD mineralogy.

Log-derived mineralogy

Concentrations of Al, Fe, and K were also measured on a continuous basis by the ERT, GST, and NGT tools. These tools respond to the average chemical content in a volume of formation that is orders of magnitude larger, and consequently more representative of the formation, than the volume of a sidewall core or core plug. If the same minimal-input model that was derived from the sidewall core data was applied to the log chemistry data, continuous logs of the estimated mineral abundances were generated.

It was first necessary to confirm that the log-derived elemental concentrations were in agreement with the neutron activation analyses of the sidewall cores. Figure 3a shows the K concentration log as a function of depth and the K concentrations measured on the sidewall core samples before and after hydrocarbon removal. This presentation is preferable to a crossplot comparison because of the problem of matching the depth of the log precisely with the depth of the sidewall core, and because of the large differences in formation volume sampled by the different techniques. Lignite zones, identified from other log data, are shown as
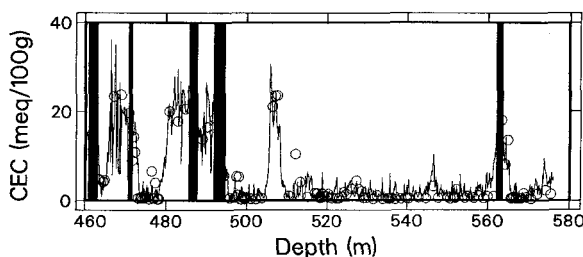
Figure 5. Cation-exchange capacity estimated from log-derived clay mineral abundances in Figure 4 (curve) and laboratory measurements on sidewall cores (circles).
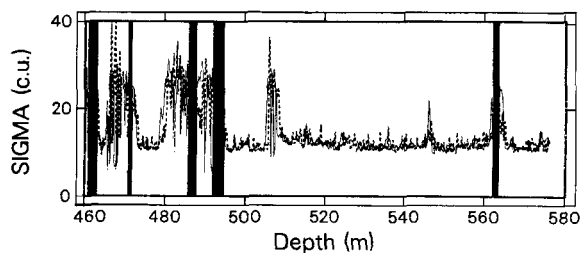

Figure 6. Sigma, the thermal neutron capture cross section, as determined from log-derived mineralogy of Figure 4 (dashed curve) and as measured by Gamma-Ray Spectroscopy Tool (solid curve). A "ringing" processing artifact is present in the measured curve in some shale (high sigma) sections.

black bands. It is clear from Figure 3a that the two techniques were in acceptable agreement. Figure 3b shows the Fe concentrations derived from the GST log and the iron concentrations measured on the sidewall cores. Figure 3c shows the agreement between Al concentrations derived from the ERT tool and those measured on the sidewall cores. These log-derived concentrations were also in generally good agreement with the neutron activation analyses.

Concentrations of Al, Fe, and K derived from the ERT, GST, and NGT logs were processed through the same element-mineral transform matrix as was used for the core data. The resulting continuous mineral abundance logs are shown in Figure 4. The mineralogy determined from XRD is also shown for comparison. Lignite zones are here also shown as black bands. Despite the exclusion of rarely observed minerals, such as pyrite and siderite, from consideration, the model mineral abundances agreed very well with the laboratory measurements. Here also, some scatter was present due to the difference in volumes sampled by core and log measurements, but overall the agreement was satisfying.

In many well operations, ten or fewer cores might be analyzed for mineralogy over a 120-m interval of interest such as this. Clearly, the log-derived mineral abundance curves were not only good estimations of the mineral abundances, but they provided remarkably detailed mineralogical information. The well could therefore be viewed on a continuous basis in terms of its constituent minerals, rather than simply in terms of the derivative lithological categories, such as sand or shale, that are normally used in formation evaluation.

Applications of log-derived mineralogy

Continuous mineral-abundance curves such as those in Figure 4 could have many applications in reservoir quality evaluation, production risk assessment, facies evaluation, and well-to-well correlation, etc., as discussed below.

Depositional environment is an important factor in predicting formation geometries and properties away from the borehole. Evaluating deltaic environments

requires knowing whether the sands were deposited in an alluvial, marine, or transitional setting. Frequently, such a distinction requires expensive and time-consuming paleontological investigations. The clay mineral assemblage can help distinguish marine, transitional, and nonmarine environments in both modern and ancient sediments (Parham, 1966; Potter *et al.,* 1980; Lonnie, 1982). Nonmarine deposits commonly contain kaolinite as the dominant clay mineral, whereas illite abundances are greater in marine deposits. The clay abundance curves in Figure 4 can be interpreted in light of these observations. Kaolinite was found to be the dominant clay mineral in the lower 80 m of the well indicating a nonmarine environment of deposition. The upper 40 m were found to be increasingly illitic suggesting a more marine, perhaps brackish environment. This interpretation is in accord with a sedimentological evaluation of the whole core from this well (Pirie and Everett, 1984) and the lone appearance of a plankton test at 483.4 m in one of the more illitic zones.

A second potential use of continuous mineral logs concerns the impact of clays on electrical conductivity, which has been linked to the CEC of the formation (e.g., Waxman and Smits, 1968). Clay minerals are major contributors to the CEC of a formation and, as a first approximation, the CEC can be approximated as a linear combination of the clay abundances. Figure 5 shows such an approximation based on the log-derived mineral abundances and assigned kaolinite and illite CEC values of 5 and 50 meq/100 g, respectively. The assigned kaolinite CEC is in line with literature values (Grim, 1968); the illite CEC is slightly higher to account for the smectite influence. This geochemically derived CEC appears to be a close approximation of the values obtained from sidewall core analysis. Note particularly the low CEC values at 546 m. This depth interval contains more than 40% clay, but has a CEC of only 3.1 meq/100 g because the clay is predominately kaolinite.

A third example concerns the thermal neutron capture cross section, also known as Σ, a common well-

logging measurement used to distinguish saline water (high Σ) from hydrocarbons (low Σ). The Σ of a formation is a simple combination of the abundance of each element in a unit volume multiplied by its known elemental cross section. The Σ of the rock, particularly if it varies with depth, is a complication to interpreting Σ logs because some of the largest contributors to a rock Σ include B and Gd for which concentration data are usually lacking. In the well examined in the present study, the Σ of the formation was approximated from a porosity log and the derived mineral abundances of Figure 4. It was assumed that each mineral had a unique capture cross section and that the pore fluids had a Σ of 22 capture units, similar to the value of pure water or oil. Figure 6 shows the Σ measured by the GST log over the interval and the approximate sigma derived from the mineralogy. A "ringing" artifact of the signal processing was unfortunately present in the data for some shales and the measured Σ does not reflect the true formation Σ. Otherwise, the measured and derived values agree, suggesting that concentrations of B, Gd, and other high-Σ elements were present in about the same proportions within the individual minerals in this well.

The agreement between measured and derived Σ curves in Figure 6 suggests that individual elemental concentrations could be modeled as simple linear combinations of the mineral abundances. In essence, each element was assumed to have a unique concentration in each mineral phase. Figure 7 shows examples of La, Th, U, Ti, Sc, and V concentrations that were derived from the mineralogy shown in Figure 4, assuming that only the clay minerals contributed to these trace element concentrations. Kaolinite and illite were assigned the elemental concentrations shown in Table 2. Also shown in Figure 7 are the neutron activation analyses of the sidewall cores before and after hydrocarbon removal. The elements La and Th were found to be associated with the kaolinite factor, which was reflected in the higher kaolinite coefficients in Table 2. Sc was found to be associated with both the kaolinite and illite factors, as reflected in the nearly equivalent coefficients. The derived and measured values showed good agreement for La (Figure 7a), Th (Figure 7b), and Sc (Figure 7c). Similarly, the measured Ti (Figure 7d) and U (Figure 7e) concentrations agreed with the derived concentrations except for a few intervals, notably at about 495 m, 515 m, 525 m, and 550 m. The factor analysis results indicated that Ti, and to a lesser extent
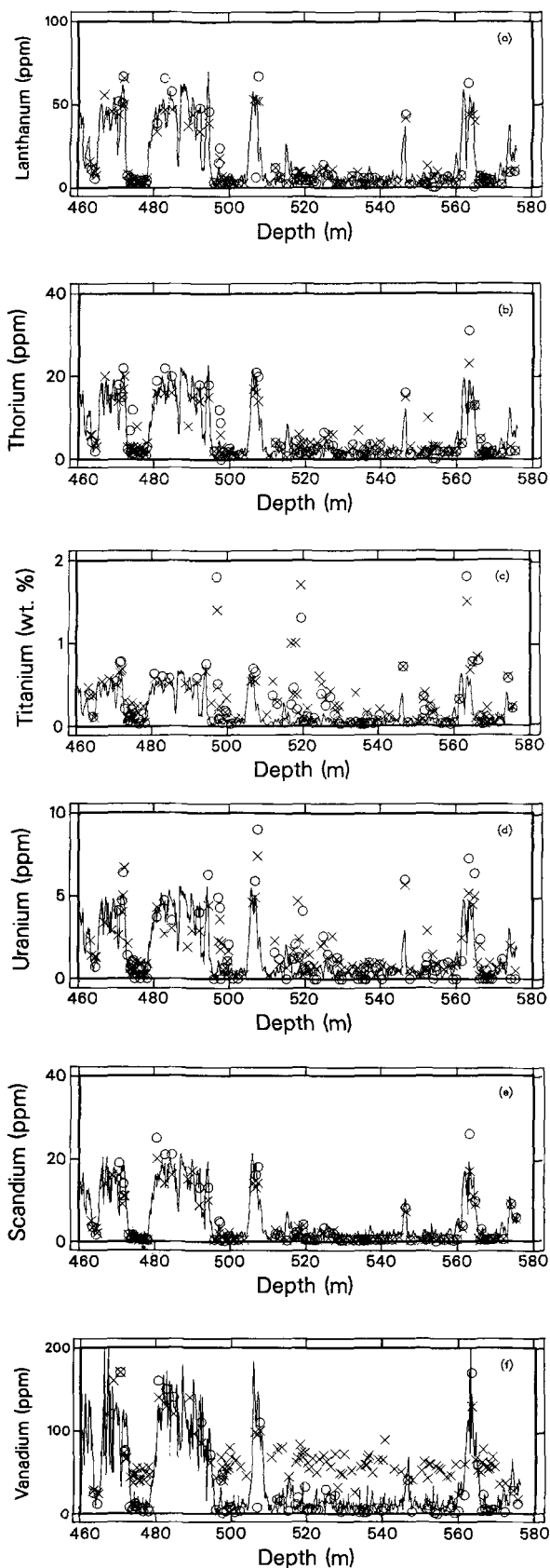
$\rightarrow$

Figure 7. Elemental concentrations estimated from log-derived clay mineralogy of Figure 4 and "end-member" coefficients in Table 2 (curve). Neutron activation analyses of sidewall cores before (crosses) and after (circles) hydrocarbon removal are shown for comparison: (a) lanthanum; (b) thorium; (c) titanium; (d) uranium; (e) scandium; (f) vanadium.

Table 2. "End-member" coefficients (ppm) for illite and kaolinite used to generate Figure 7, and measured values on poorly ordered and well-ordered Georgia kaolinites before (A) and after (B) cation exchange.

Element	Venezuela		Poorly ordered kaolinites		Well-ordered kaolinites	
	Illite	Kaolinite	A	B	A	B
La	35	85	79 ± 4	77 ± 7	13 ± 9	14 ± 11
Th	17	27	23 ± 6	23 ± 4	45 ± 26	48 ± 32
Ti	4000	9000	9000 ± 3000	9000 ± 3000	14,000 ± 8000	14,000 ± 8000
U	4.5	6.7	6.7 ± 1.2	6.2 ± 1.0	4.0 ± 1.6	3.9 ± 1.3
Sc	20	23	26.5 ± 1.0	25.5 ± 1.3	31 ± 6	31 ± 9
V	220	120	158 ± 5	155 ± 6	255 ± 69	243 ± 69

U, correlated with Hf concentrations, which are also relatively large in these same intervals. These results suggest that the clay contribution was well described by the derived curves, but that an additional heavy mineral source of Ti and U was present in other samples.

Figure 7f shows derived and measured concentrations of V, an element primarily associated with the illite factor. The derived curve closely approximated the concentrations in shales, in sands with the hydrocarbons removed, and in the water-bearing sand at 465 m. In contrast, hydrocarbon-bearing samples, such as the sand zone at about 495 m to 505 m depth, contained an additional vanadium contribution from the heavy oil. This excess V, adjusted for the volume of hydrocarbon, was converted to a concentration in the oil of 400 ppm, which compares well with the 390 ppm measured on a single sample of the heavy oil. Total V concentrations, uncorrected for the mineral-derived V, would be unsuitable for such calculations; indeed, the highest total V concentrations were in the shales. V concentrations in heavy oils have been used as indicators of the API Gravity, or viscosity, of heavy oils (e.g., Kapo, 1978).

Applicability in other geologic settings

From the minimal-input model, it was possible to approximate the mineralogy, CEC, Σ, and additional elements from concentrations of Al, Fe, and K in a Venezuelan deltaic system. Similar studies, involving core calibration of the relationship between chemistry and mineralogy, could, of course, be undertaken in other areas of the world. On the other hand, it is desirable to learn the applicability of this particular model in other areas of the world with the same limited mineral suite and the applicability of an expanded model in areas with more complex mineralogies. The model is based on two assumptions: (1) The elemental concentrations in each mineral phase are constant, and (2) No other minerals are present, such as pyrite or chlorite, that contain Al, Fe, or K. The agreement between derived and measured mineral abundances indicates that these assumptions were generally valid for this well. The agreement between measured and modeled trace element concentrations suggests that the first

assumption was valid even beyond the major elements used in the minimal-input model.

The applicability of the model in a geological environment where the clay mineralogy is still largely limited to kaolinite and illite is discussed below: Figure 8 shows the abundances of kaolinite and illite relative to total clay in samples from clay beds on Long Island (Lonnie, 1982). These samples were deposited under conditions ranging from nonmarine to marine and show correlations between clay mineralogy and depositional environment that are similar to those observed in the MFM-7S well. Nonmarine clays were dominantly kaolinitic, marine clays were more illitic and contained some chlorite and mixed-layer phases, and clays deposited in a transitional environment were intermediate in composition. Figure 8 also shows the relative kaolinite and illite abundances derived from the minimal-input model using the Al, Fe, and K concentrations given by Lonnie (1982). The agreement was good for samples which contained only those minerals for which the model was designed, as in the nonmarine and transitional samples, despite the differences in provenance and age. The Long Island samples were of Cretaceous and Pleistocene age, whereas the Venezuelan samples used in constructing the model were of Miocene age (Lonnie, 1982; Pirie and Everett, 1984).

The major deviations appear to have been due to the presence of minerals not accounted for in the minimal-input model, particularly in the marine clays, rather than varying chemical composition of the clays. Chlorite and mixed-layer phases, which were abundant in the Monmouth Group samples and present in the Pleistocene samples, resulted in an overestimation of the illite abundance. The degree of agreement in the other Long Island samples, however, indicates that the minimal-input model is not restricted in applicability to the Oficina Formation or to Venezuela.

A more complex mineral suite will require an expansion of the model to include more elemental inputs as well as more mineral outputs. Si and Ca, for example, may be added as input variables and quartz and calcite as output minerals. These elements can be measured with geochemical logging tools such as the GST and ERT. The problem with adding new mineral phases is that they must obey the assumption that the el-

emental composition of each phase is constant. This assumption is widely believed to be invalid, particularly for the clay minerals (Weaver and Pollard, 1975) and especially for the trace elements in clays. Cody (1971) listed eight factors that influence adsorption and fixation processes and, consequently, clay composition: (1) dissolved adsorbate concentration, (2) temperature, (3) pH, (4) kind and amount of dissolved inorganic and organic substances other than the adsorbate, (5) surface area of the clay adsorbent, (6) crystalline structure of the adsorbent, (7) time, and (8) drying state of the clays after initial sorption. The fact that the concentrations of La, Th, Sc, V, and, indeed, all elements primarily associated with factors 1 and 4, were approximated by assuming a unique concentration for the clay phases is somewhat surprising, given this list of parameters.

The observed trace element-clay correlations may possibly be controlled by the variables relating to adsorption, and the effects of these factors may be overall fairly uniform for all the samples in the well, due to a similar provenance and geologic history. If this explanation accounts for the observed correlations, the quantities of each trace element adsorbed onto individual clay minerals should reflect the surface area or CEC of the clays; i.e., higher amounts should be adsorbed on the illite compared to the kaolinite. In addition, because the shales with higher illite abundances were deposited under apparently more saline conditions than were the alluvial, kaolinite-rich shales, the effect of higher solute concentrations as well as pH should favor greater trace element concentrations in the illite phase. Five of the six sets of coefficients in Table 2, however, are greater for the kaolinite than for illite, suggesting that adsorption was not the dominant process responsible for the trace element-clay correlations.

Alternatively, ion fixation within the structure, rather than adsorption, governed the final trace element concentrations. Decarreau (1985) showed that concentrations of transition metals in smectites can be explained in terms of normal partition coefficients between the fluid phase and octahedral sites, the value of the partition coefficient being dependent on the particular metal. A similar relationship may be expected for other clays; of the factors listed by Cody (1971), the influence of "crystallinity" or the degree of disorder in the structure should then overwhelm the effects of other parameters in determining concentrations in different clay phases. Several authors have found a correlation between the degree of disorder and the small quantity of structural iron in kaolinites deposited under a wide variety of geologic conditions (e.g., Mestdagh et al., 1980; Brindley et al., 1986). Apparently, the various geologic factors that impact the Fe concentrations are of secondary importance to the degree of disorder in the structure. A similar situation is possible
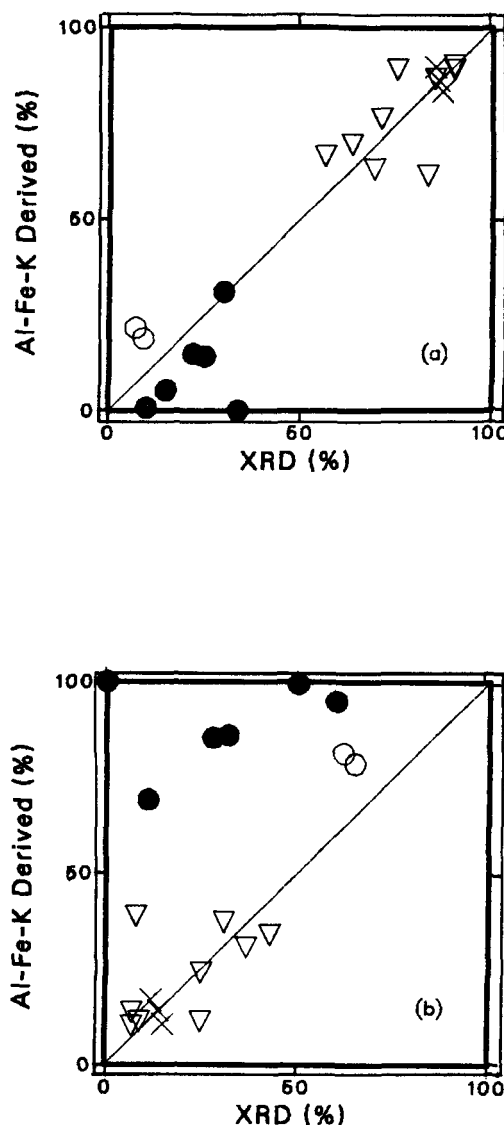

Figure 8. Clay mineralogy of Long Island samples as reported by Lonnie (1982) and as calculated from minimal-input model and Al, Fe, and K concentrations. Samples represent Pleistocene marine (open circles), Monmouth Group marine (solid circles), nonmarine (crosses), and transitional (triangles) depositional environments: (a) kaolinite; (b) illite.

for the significantly lower concentrations of at least some trace elements. If so, other clay phases with similar degrees of disorder should have similar trace element concentrations to those in Table 2.

The Venezuelan kaolinites have crystallinity indexes (Hinckley, 1963) of about 0.5, indicating a high degree of disorder. Four samples of Georgia kaolinites with comparable crystallinity indexes (0.41–0.57) and four with high indexes (1.21–1.57) were analyzed twice by neutron activation. The first analysis was of the samples as received; the second was of aliquots in which

all exchangeable cations had been replaced by NH_4^+. Table 2 shows the means and standard deviations of the La, Th, U, Ti, Sc, and V concentrations of these samples. Concentrations of these elements and, indeed, all detected trace elements, were not affected by the ion-exchange procedure within the measurement error. These elements were not exchangeable, although they may have been fixed after an initial adsorption. The well-ordered samples differed significantly in composition from the poorly ordered samples. Remarkably, the concentrations in the poorly ordered Georgia kaolinites were very similar to the values used to generate the curves of Figure 7 for the Venezuelan kaolinites. The thorium concentrations of the Georgia kaolinites were also similar to values reported for Wyoming kaolinites characterized by diffuse (25.5 ppm Th) and sharp (42 ppm Th) XRD patterns (Adams and Weaver, 1958). These results lend some support to the explanation that the concentrations may have been significantly affected by the degree of disorder.

If trace element concentrations in clays primarily reflect the degree of structural disorder, the idea of a generally applicable element-mineral transform may be feasible. It may be possible, for example, to measure elements which are diagnostic of clay disorder, such as La or V, in addition to the elements needed to estimate the mineral abundances. In such an over-determined system, the outputs could include degree of clay disorder as well as type and amount of each phase, and thus may provide a means of distinguishing authigenic from detrital phases.

SUMMARY AND CONCLUSIONS

Multivariate statistical analysis of combined geochemical and mineralogical sidewall-core data in the MFM-7S well has demonstrated clear relationships between elemental concentrations and mineral abundances. Four factors accounted for most of the observed variance. Three of these factors are quantitatively related to the major mineral phases in the core; a fourth factor is believed to be related to heavy mineral abundances. The element-mineral transform matrix operation is, in some respects, similar to the more conventional normative mineral analysis (see, e.g., Imbrie and Poldervaart, 1959), but treats variables collectively rather than sequentially. Mineral abundances derived from this operation are in good agreement with XRD determinations and permit calculation of many petrophysical parameters which may be considered as linear combinations of the mineral concentrations. As an example, cation-exchange capacity may be estimated as a linear combination of the clay mineral phases present. Another example important in well logging is the matrix Σ, estimated as a volume-normalized linear combination of the minerals present. Similarly, the V content of the minerals may be modeled as a linear combination of the minerals present. If mineral V is

subtracted from the total V concentration, V due to the heavy oil can be calculated and converted into the API Gravity of the oil.

The same type of statistical analysis of the mineral-element correlations to generate a valid deterministic model can be applied to wells in other basins of the world. The model can then be applied to log-derived geochemical data to generate a detailed evaluation of similar wells in the area.

The minimal-input model used in this study has clear limitations. Even in this relatively uncomplicated well, important mineral phases were not taken into account; however, the concept is not limited to the few variables used; many more variables are available from both neutron activation data and the geochemical logs. The ability to model concentrations of many of these elements in conditions of simple mineralogy indicates that they may eventually be used as inputs for geochemical models of more complex mineralogical systems.

The results of this study indicate that much of the observed variability in chemical concentrations in clays may be understandable largely in terms of trace, but chemically significant, minerals such as zircon, and the effects of structural disorder. The clay mineralogy of Long Island samples can be fairly well approximated using the minimal-input model developed on Venezuelan samples; the greatest discrepancies occur for samples containing minerals not included in the model. The concentrations of most trace elements in this well can be successfully modeled as linear combinations of the clay mineral abundances. The "end-member" coefficients used for kaolinite are similar to values measured in Georgia kaolinites of similar degrees of disorder. The trace elements in the Georgia samples are not exchangeable. These observations can be most simply explained in a working hypothesis that the average chemical composition, including all elements, of sedimentary minerals of a given degree of structural disorder is fairly uniform.

ACKNOWLEDGMENTS

REFERENCES

Adams, J. A. S., Osmond, J. K., and Rogers, J. J. W. (1959) The geochemistry of thorium and uranium: *Phys. Chem. Earth* **3**, 298–348.
Adams, J. A. S. and Weaver, C. E. (1958) Thorium-to-uranium ratios as indicators of sedimentary processes: example of concept of geochemical facies: *Bull. Amer. Assoc. Pet. Geol.* **42**, 387–430.
Brindley, G. W., Kao, C-C., Harrison, J. L., Lipsicas, M., and

Raythatha, R. (1986) The relation between structural disorder and other characteristics of kaolinites and dickites: *Clays & Clay Minerals* **34** (in press).

Cody, R. D. (1971) Adsorption and the reliability of trace elements as environmental indicators for shales: *J. Sediment. Petrol.* **41**, 461–471.

Davis, J. C. (1973) *Statistics and Data Analysis in Geology:* Wiley, New York, 473–533.

Decarreau, A. (1985) Partitioning of divalent transition elements between octahedral sheets of trioctahedral smectites and water: *Geochim. Cosmochim. Acta* **49**, 1537–1544.

Everett, R., Herron, M., and Pirie, G. (1983) Log responses and core evaluation case study technique: field and laboratory procedures: Soc. Prof. Well Log Analysts Ann. Meet., Calgary, Alberta, 1983, Paper OO.

Gold, C. M., Cavell, P. A., and Smith, D. G. W. (1983) Clay minerals in mixtures: sample preparation, analysis, and statistical interpretation: *Clays & Clay Minerals* **31**, 191–199.

Grim, R. E. (1968) *Clay Mineralogy:* McGraw-Hill, New York, 185–233.

Hinckley, D. N. (1963) Variability in "crystallinity" values among the kaolin deposits of the coastal plain of Georgia and South Carolina: in *Clays and Clay Minerals, Proc. 11th Natl. Conf., Ottawa, Ontario, 1963,* W. F. Bradley, ed., Pergamon Press, New York, 229–235.

Hodgson, M. and Dudeney, A. W. L. (1984) Estimation of clay proportions in mixtures by X-ray diffraction and computerized chemical mass balance: *Clays & Clay Minerals* **32**, 19–28.

Imbrie, J. and Poldervaart, A. (1959) Mineral compositions calculated from chemical analyses of sedimentary rocks: *J. Sediment. Petrol.* **29**, 588–595.

Kapo, G. (1978) Vanadium: key to Venezuelan fossil hydrocarbons: in *Bitumen, Asphalts, and Tar Sands,* G. V. Chilingarian and T. F. Yen, eds., Elsevier, Amsterdam, 213–241.

Lonnie, T. P. (1982) Mineralogic and chemical comparison of marine, nonmarine, and transitional clay beds on south shore of Long Island, New York: *J. Sediment. Petrol.* **52**, 529–536.

Mestdagh, M. M., Vielvoye, L., and Herbillon, A. J. (1980) Iron in kaolinite: II. The relationship between kaolinite crystallinity and iron content: *Clay Miner.* **15**, 1–13.

Miesch, A. T. (1962) Computing mineral compositions of sedimentary rocks from chemical analyses: *J. Sediment. Petrol.* **32**, 217–225.

Murali, A. V., Parthasarathy, R., Mahadevan, T. M., and Sankar Das, M. (1983) Trace element characteristics, REE patterns and partition coefficients of zircons from different geological environments—a case study on Indian zircons: *Geochim. Cosmochim. Acta* **47**, 2047–2052.

Parham, W. E. (1966) Lateral variations of clay mineral assemblages in modern and ancient sediments: in *Proc. Int. Clay Conf., Jerusalem, 1966, Vol. 1,* L. Heller and A. Weiss, eds., Israel Prog. Sci. Transl., Jerusalem, 135–145.

Pearson, M. J. (1978) Quantitative clay mineralogical analyses from the bulk chemistry of sedimentary rocks: *Clays & Clay Minerals* **26**, 423–433.

Pirie, G. and Everett, R. (1984) Depositional environments and invasion profiling in heavy oil sands, eastern Venezuela: a case study: *Amer. Assoc. Petrol. Geol. Bull.* **68**, 516 (abstract).

Potter, P. E., Maynard, J. B., and Pryor, W. A. (1980) *Sedimentology of Shale:* Springer-Verlag, New York, 303 pp.

Rankama, K. and Sahama, T. G. (1950) *Geochemistry:* University of Chicago Press, Chicago, 557–569.

Ridge, M. J. (1983) A combustion method for measuring the cation exchange capacity of clay materials: *Log Analyst* **24**, 6–11.

Tardy, Y. (1975) Element partition ratios in some sedimentary environments: *Sci. Geol. Bull.* **28**, 59–73.

Turekian, K. K. and Wedepohl, K. H. (1961) Distribution of the elements in some major units of the earth's crust: *Geol. Soc. Amer. Bull.* **72**, 175–192.

Waxman, M. H. and Smits, L. J. M. (1968) Electrical conductivities in oil-bearing shaly sands: *Soc. Prof. Eng. J.* **243**, 107–122.

Weaver, C. E. and Pollard, L. D. (1975) *The Chemistry of Clay Minerals:* Elsevier, Amsterdam, 205 pp.